# Tuning the response of magnetic suspensions

M. Chen and L. Sun
*Department of Materials Science and Engineering, Johns Hopkins University, Baltimore, Maryland 21218*

J. E. Bonevich
*Metallurgy Division, National Institute of Standards and Technology, Gaithersburg, Maryland 20899*

D. H. Reich and C. L. Chien
*Department of Physics and Astronomy, Johns Hopkins University, Baltimore, Maryland 21218*

P. C. Searson[a)]
*Department of Materials Science and Engineering, Johns Hopkins University, Baltimore, MD 21218*

(Received 23 January 2003; accepted 27 February 2003)

Electrochemical template synthesis of multilayer nanowires consisting of alternating ferromagnetic and nonmagnetic layers provides an approach to control the properties of magnetic particles in suspension. Copper/nickel multilayer nanowires were fabricated by electrochemical deposition from a solution containing both nickel and copper ions. We demonstrate that the magnetic shape anisotropy and dipolar interactions between magnetic layers can be exploited to tailor the magnetic response in ferromagnetic/nonmagnetic multilayer nanowires in a suspension. © *2003 American Institute of Physics.* [DOI: 10.1063/1.1569429]

Suspensions of superparamagnetic particles are of interest in applications such as ferrofluidics[1,2] and biomagnetics.[3,4] In contrast to the spherical particles commonly used in these applications, rod-shaped particles such as nanowires exhibit additional degrees of freedom that are associated with their inherent shape anisotropy. Furthermore, the introduction of multiple components along the length of a nanowire can lead to further degrees of freedom associated with the magnetic coupling between the layers. By modifying the diameter, composition, and layer thicknesses in multilayer nanowires, it is possible to tailor properties such as the magnetic easy axis, coercivity, saturation field, saturation magnetization, remanent magnetization, and the Curie temperature. Here, we demonstrate that the magnetic shape anisotropy and dipolar interactions between magnetic layers can be exploited to tailor the magnetic response in ferromagnetic/nonmagnetic (FM/NM) multilayer nanowires in a suspension.

Fabrication of multilayer nanowires is achieved by electrochemical template synthesis.[5,6] Template synthesis is preferred over other techniques since it is easily adapted for the deposition of multilayer nanowires from a single solution. Furthermore, template synthesis can produce large quantities of nanowires with monodisperse size.

Compositionally modulated multilayer with bilayer repeat units of the form $A_xB_{1-x}/A_yB_{1-y}$ can be electrodeposited from a single solution containing the ions of the two components by modulating the deposition potential.[7–11] For the case where the difference in equilibrium potentials of A and B is sufficiently large (typically $>0.4$ V) and the concentration of the more noble component is very low (i.e. $[A^{n+}] \ll [B^{m+}]$), multilayers of the form $A_xB_{1-x}/A$ with $x \approx 0.01$ can be deposited. In this case, A (e.g., Cu) is deposited at more positive potentials and an $A_xB_{1-x}$ alloy (e.g., $Cu_xNi_{1-x}$) is deposited at more negative potentials.

Figure 1 shows a current versus voltage curve for 0.5 mol/L $NiSO_4$ + 0.005 mol/L $CuSO_4$ + 0.6 mol/L $H_3BO_3$ on a gold film. The equilibrium potentials for copper and nickel in this solution are 0.15 V (versus Ag/AgCl) and $-0.468$ V (versus Ag/AgCl), respectively. On scanning the potential negative from the open-circuit potential, the current onset at about $+0.05$ V is followed by a peak associated with the nucleation and growth of copper. At more negative potentials, the onset of nickel deposition is seen at about $-0.7$ V. On the reverse scan, the diffusion limited deposition of copper is seen up to about 0 V followed by a peak associated with the stripping of copper.[8]

Ni/Cu multilayer nanowires were fabricated by electrodeposition into 6 $\mu$m thick nanoporous polycarbonate membranes with pore sizes in the range 30 to 100 nm by modulating the potential between $-1.0$ V and $-0.16$ V (ver-

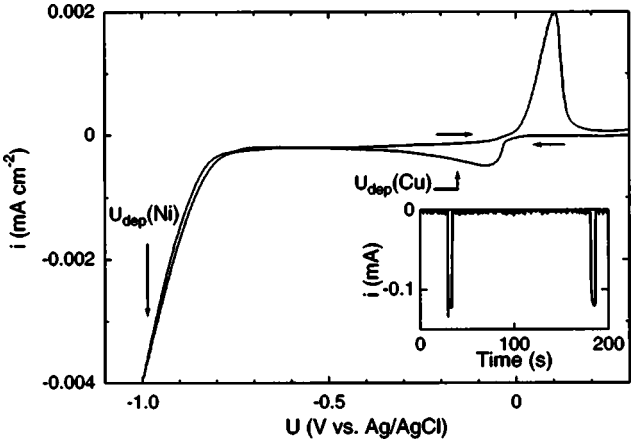


FIG. 1. Current–voltage curve for 0.5 mol/L $NiSO_4$ + 0.005 mol/L $CuSO_4$ + 0.6 mol/L $H_3BO_3$ on a gold film at 10 mV s$^{-1}$. The inset shows part of a current–time curve for the deposition $[Ni(125\ nm)/Cu(125\ nm)]_{10}$ $d$ = 50 nm multilayer nanowires. The two short ($\approx$4 s) sections correspond to the deposition of Ni at $-1.0$ V whereas the longer ($\approx$140 s) section corresponds to the deposition of Cu at $-0.16$ V.

a)Author to whom correspondence should be addressed; electronic mail: searson@jhu.edu

 

sus Ag/AgCl). Pure Cu is deposited at $-0.16$ V since this is the positive of the equilibrium potential for Ni. At $-1.0$ V, both Ni and Cu are deposited with a composition of $Cu_{0.1}Ni_{0.9}$.[12]

In order to ensure reproducible layer thicknesses the potential was switched when the charge reached a value corresponding to the required layer thickness. The inset of Fig. 1 shows part of a current–time transient for the deposition of 50 nm diameter $[Ni(125\ nm)/Cu(125\ nm)]_{10}$ multilayer nanowires.

Figure 2 shows transmission electron microscope images of Ni/Cu multilayer nanowires. The top image in Fig. 2 shows a bright-field image of a 130 nm diameter [Ni(20 nm)/Cu(10 nm)] multilayer nanowire. The disk-shaped nickel (dark) and copper (light) segments are clearly distinguished. The middle image in Fig. 2 shows an electron energy loss spectroscopy map of two 30 nm diameter [Ni(5 nm)/Cu(5 nm)] multilayer nanowires. The lower image shows an electron energy loss spectroscopy map of a 30 nm diameter [Ni(1.5 nm)/Cu(4 nm)] multilayer nanowire. These images illustrate the reproducible layer structure and sharp interfaces that can be achieved with this technique.

The magnetic properties of FM/NM multilayer nanowires can be precisely tuned by varying the size, aspect ratio, and spacing of the FM segments. Manipulation of the magnetic shape anisotropy and intersegment dipolar interactions allows many effects to be exploited. Figure 3 shows magnetization curves for arrays of Ni/Cu multilayer nanowires at 25 K. Figure 3(a) shows the magnetic response of $[Ni(125\ nm)/Cu(125\ nm)]_{10}$ $d=50$ nm nanowires with rod-shaped nickel segments (aspect ratio 2.5). For rod-shaped magnetic segments, the easy axis is parallel to the nanowire axis. The segments are single domain in this size regime and exhibit large coercivity and remanence due to the inherent shape anisotropy and reduced dimensions.[13,14] In contrast, the axis perpendicular to the nanowire axis is the magnetic hard axis with small coercivity and remanence.

The coercivity and remanence along the easy axis are dependent on the nanowire diameter and hence can be tuned by the selection of the appropriate nanowire dimensions. The coercivity increases with decreasing nanowire diameter, and can reach values close to 79 kA/m ($\approx 1$ kOe) for Ni nanowires 30 nm in diameter.[15] The remanence also increases with decreasing nanowire diameter and values as large as 0.96 have been obtained for well-aligned Ni nanowires.[15] We also note that the Curie temperature decreases with decreasing nanowire diameter[16] and hence can be used to tailor the magnetic response.

Figure 3(b) shows magnetization curves for $[Ni(5\ nm)/Cu(5\ nm)]_{250}$ $d=50$ nm nanowires with disk-shaped nickel segments (aspect ratio 0.1). In this case, the magnetic easy axis is perpendicular to the nanowire axis and the hard axis is parallel to the nanowire axis. The remanence is very small due to the dipolar interactions between adjacent FM layers. The remanence can be tuned by adjusting the copper layer thickness, as shown in the inset in Fig. 3(b). Dipolar interactions between the magnetic segments favor antiparallel alignment of the domains in adjacent nickel segments. As the copper layer thickness increases, the remanence increases as the dipolar interactions become weaker.

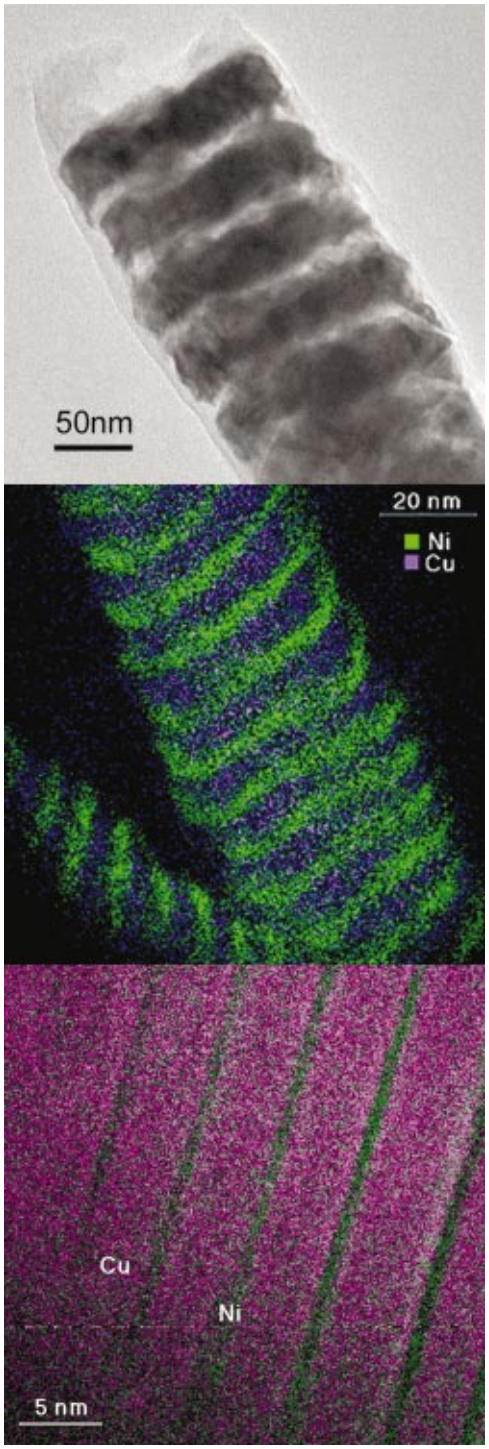


FIG. 2. (Color) Transmission electron microscopy images of Ni/Cu multilayer nanowires: (top) Bright-field image of a $[Ni(20\ nm)/Cu(10\ nm)]_n$ $d=130$ nm nanowire, (middle) electron energy loss spectroscopy map of portions of two [Ni(5 nm)/Cu(5 nm)] $d=30$ nm nanowires, and (bottom) electron energy loss spectroscopy image of part of a [Ni(1.5 nm)/Cu(4 nm)] $d=30$ nm nanowire.

Magnetic interactions between particles in a suspension can influence the stability of the suspension and can be exploited in the assembly of larger scale structures. For example, rod-shaped magnetic nanowires with high remanence can act as small bar magnets in a suspension and form one-dimensional chains due to the attractive wire–wire interactions.[17] In multilayer FM/NM nanowires, the remanence is dependent on the aspect ratio and thickness of the

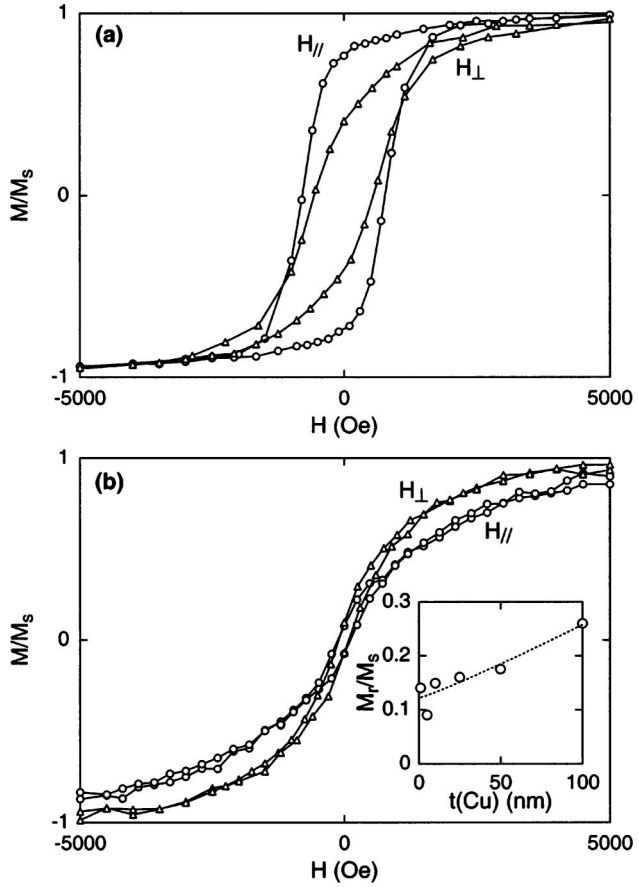


FIG. 3. $M-H$ loops for arrays of Ni/Cu multilayer nanowires in the template at 25 K: (a) $[\mathrm{Ni}(125\ \mathrm{nm})/\mathrm{Cu}(125\ \mathrm{nm})]_{10}$, $d=50$ nm, and (b) $[\mathrm{Ni}(5\ \mathrm{nm})/\mathrm{Cu}(5\ \mathrm{nm})]_{250}$, $d=50$ nm. In (a), the nanowires have rod-shaped FM segments (aspect ratio 2.5) and the easy axis is parallel to the wire axis. In (b), the nanowires have disk-shaped FM segments (aspect ratio 0.1) and the easy axis is perpendicular to the wire axis. The inset shows the remanence for $[\mathrm{Ni}(5\ \mathrm{nm})/\mathrm{Cu}(\mathrm{X}\ \mathrm{nm})]$ $d=50$ nm nanowires as a function of the thickness of the copper layer.

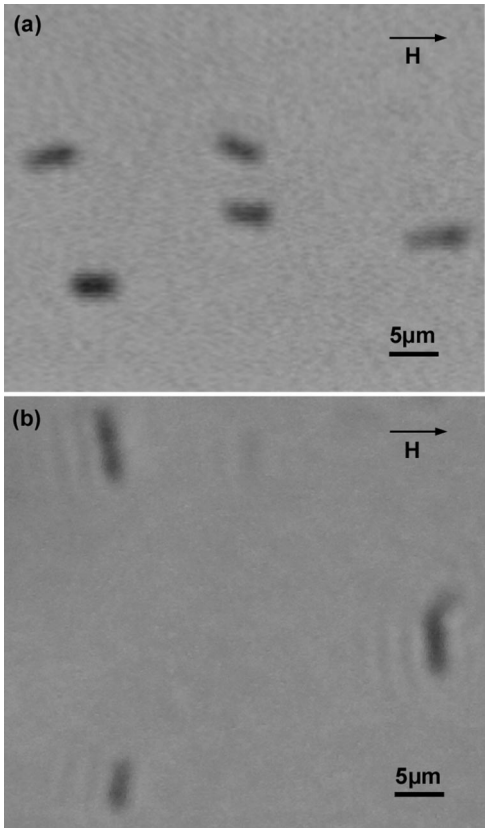


FIG. 4. Optical microscope images of Ni/Cu multilayer nanowires suspended in a 1:1 octadecane and hexdecane mixture under an externally applied magnetic field. In both cases, the nanowires are 100 nm in diameter and about 6 $\mu$m long with an average composition of 50 at. % nickel, (a) $[\mathrm{Ni}(1000\ \mathrm{nm})/\mathrm{Cu}(1000\ \mathrm{nm})]_3$ $d=100$ nm and (b) $[\mathrm{Ni}(10\ \mathrm{nm})/\mathrm{Cu}(10\ \mathrm{nm})]_{300}$ $d=100$ nm.

FM and NM layers allowing control of aggregation and assembly.

The response of multilayer FM/NM nanowires in a suspension to a small magnetic field can also be tailored by controlling the aspect ratio and thickness of the FM and NM layers. Figure 4 shows suspensions of Ni/Cu multilayer nanowires in a small ($\approx 0.8$ kA/m, or 10 Oe) external magnetic field. Figure 4(a) shows $[\mathrm{Ni}(1000\ \mathrm{nm})/\mathrm{Cu}(1000\ \mathrm{nm})]_3$ $d=100$ nm nanowires with rod-shaped FM segments. The nanowires align parallel to the applied magnetic field since the easy axis is parallel to the wire axis. Figure 4(b) shows $[\mathrm{Ni}(10\ \mathrm{nm})/\mathrm{Cu}(10\ \mathrm{nm})]_{300}$ $d=100$ nm nanowires with disk-shaped FM segments. The nanowires have the same overall length and the same amount of nickel as the nanowires with the rod-shaped FM segments shown in Fig. 4(a), however, these nanowires align perpendicular to the applied field since the easy axis is perpendicular to the wire axis.

In summary, the synthesis of multilayer FM/NM nanowires provides an approach to control the properties of magnetic particles in suspension. Properties such as the magnetic easy axis, Curie temperature ($T_C$), coercivity ($H_C$), and remanent magnetization ($M_R$) can be tailored by controlling the composition and dimensions of the FM and NM segments.

This work was supported by the JHU MRSEC (DMR-0080031), the David and Lucile Packard Foundation (Grant No. 2001-17715), and DARPA/AFOSR (Grant No. F49620-02-1-0307).

[1] R. E. Rosensweig, *Ferrohydrodynamics* (Dover, New York, 1998).
[2] E. Blums, A. Cebers, and M. M. Maiorov, *Magnetic Fluids* (de Gruyter, New York, 1997).
[3] *Scientific and Clinical Applications of Magnetic Carriers*, edited by U. Hafeli, W. Schutt, J. Teller, and M. Zborowshi (Plenum, New York, 1997).
[4] *Magnetism in Medicine*, edited by W. Andra and H. Nowak (Wiley, Berlin, 1998).
[5] T. M. Whitney, J. S. Jiang, P. C. Searson, and C. L. Chien, Science **261**, 316 (1993).
[6] C. R. Martin, Science **266**, 1961 (1994).
[7] D. S. Lashmore and M. P. Dariel, J. Electrochem. Soc. **135**, 1218 (1988).
[8] D. M. Tench and J. T. White, J. Electrochem. Soc. **137**, 3061 (1990).
[9] L. Piraux, J. M. George, J. F. Despres, C. Leroy, E. Ferain, R. Legras, K. Ounadjela, and A. Fert, Appl. Phys. Lett. **65**, 2484 (1994).
[10] A. Blondel, J. P. Meier, B. Boudin, and J.-P. Ansermet, Appl. Phys. Lett. **65**, 3019 (1994).
[11] K. Liu, K. Nagodawithana, P. C. Searson, and C. L. Chien, Phys. Rev. B **51**, 7381 (1995).
[12] M. Chen and P. C. Searson (unpublished).
[13] C. A. Ross, M. Hwang, M. Shima, J. Y. Cheng, M. Farhoud, T. A. Savas, H. I. Smith, W. Schwarzacher, F. M. Ross, M. Redjdal, and F. B. Humphrey, Phys. Rev. B **65**, 144417 (2002).
[14] H. Zeng, R. Skomski, L. Menon, Y. Liu, S. Bandyopadhyay, and D. J. Sellmeyer, Phys. Rev. B **65**, 134426 (2002).
[15] L. Sun, P. C. Searson, and C. L. Chien, Appl. Phys. Lett. **74**, 2803 (1999).
[16] L. Sun, C. L. Chien, and P. C. Searson, Phys. Rev. B **61**, R6463 (2000).
[17] L. Bauer, M. Tanase, A. Hultgren, L. Sun, P. C. Searson, D. H. Reich, and G. J. Meyer, Nano Lett. **1**, 155 (2001).